

**United States  
Department of  
Agriculture**

**Natural  
Resources  
Conservation  
Service**

**c/o USDA Forest Service  
11 Campus Boulevard  
Suite 200  
Newtown Square, PA 19073  
(610) 557-4233; FAX: (610) 557-4200**

**Subject:** SOI – Geophysical Field Assistance

**Date:** 29 March 2006

**To:** Robin Heard  
State Conservationist  
USDA-NRCS,  
One Credit Union Place  
Suite 340  
Harrisburg, PA 17110-2993

**Purpose:**

The 18th World Congress of Soil Science (WCSS) will be held in Philadelphia, Pennsylvania, on July 9-15, 2006. Mid-Congress tours are being planned for Wednesday (July 12, 2006) of that week. Field work discussed in this trip report will be used for Mid-Congress Tour 20 - *New Frontiers in Soil Survey*. The MLRA Soil Survey Project Office in Leesport will demonstrate innovated methods and technologies that are being used to update and maintain soil surveys on a Land Resource Area basis. Demonstrations will include soil survey field data collection using ground-penetrating radar (GPR) and electromagnetic induction (EMI).

**Participants:**

John Chibirka, Soil Scientist, USDA-NRCS, Leesport, PA  
Jim Doolittle, Research Soil Scientist, USDA-NRCS-NSSC, Newtown Square, PA  
Vicki Meyers, Soil Scientist, USDA-NRCS, Leesport, PA  
Greg Stricker, Agricultural Engineer, USDA-NRCS, Leesport, PA  
Wes Tuttle, Soil Scientist (Geophysical), USDA-NRCS-NSSC, Wilkesboro, NC

**Activities:**

All field activities were completed during on 13 March 2005.

**Results:**

1. The surveyed areas have low and comparatively invariable  $EC_a$  and are considered poorly suited to high-intensity, EMI soil surveys. In areas of Berks and Weikert soils that are underlain by shales of the Hamburg sequence,  $EC_a$  was exceedingly low resulting in indistinct spatial patterns and ambiguous interpretations. In areas of Berks, Duffield, and Weikert soils that contain larger amounts of limestone fragments,  $EC_a$ , though low, was higher than in areas dominated by shales. Here discernible patterns were noticeable, which conformed to systematic changes in soils and landscape components.
2. Areas of Weikert and Berks soils are considered well suited to GPR. The moderate clay content and low cation-exchange capacity of these soils result in modest rates of signal attenuation that do not limit GPR for soil investigations. Ground-penetrating radar provides an effective tool for bedrock determinations in areas of Berks and Weikert soils.

It was our pleasure to work in Pennsylvania and with members of your fine staff.

With kind regards,

James A. Doolittle  
Research Soil Scientist  
National Soil Survey Center

Wes Tuttle  
Soil Scientist (Geophysical)  
National Soil Survey Center

cc:

- B. Ahrens, Director, National Soil Survey Center, USDA-NRCS, Federal Building, Room 152, 100 Centennial Mall North, Lincoln, NE 68508-3866
- S. Carpenter, MLRA Office Leader, USDA-NRCS, 75 High Street, Room 301, Morgantown, WV 26505
- J. Chibirka, Resource Soil Scientist, USDA-NRCS, Berks County Ag. Center, P.O. Box 520, Leesport, PA 19533-0520
- M. Golden, Director, Soil Survey Division, USDA-NRCS, Room 4250 South Building, 14th & Independence Ave. SW, Washington, DC 20250
- D. Hammer, National Leader, Soil Survey Investigations, National Soil Survey Center, USDA-NRCS, Federal Building, Room 152, 100 Centennial Mall North, Lincoln, NE 68508-3866
- W. Tuttle, Soil Scientist (Geophysical), USDA-NRCS-NSSC, P.O. Box 60, Federal Building, Room G-08, 207 West Main Street, Wilkesboro, NC 28697
- E. White, State Soil Scientist, USDA-NRCS, One Credit Union Place, Suite 340, Harrisburg, PA 17110-2993

### **Background:**

The Soil Survey Division of the United States Department of Agriculture-Natural Resources Conservation Service uses two noninvasive geophysical tools to support soil survey operations and investigations. These tools are electromagnetic induction (EMI) and ground-penetrating radar (GPR).

Electromagnetic induction measures the apparent conductivity ( $EC_a$ ) of soils. Apparent conductivity is a measure of the soil's ability to conduct electrical current and is primarily controlled by water, clay and soluble salts contents. Apparent conductivity provides a relational reference frame to infer and map variations in soils and soil properties. Stafford (2000) observed that  $EC_a$  is often a good substitute for a spatially varying soil property that is not easily sensed or mapped such as clay or moisture content. However, a weakness of this interpretative process is equivalence: soil properties are spatiotemporally variable and variations in two or more properties may cause equivalent EMI responses. In many landscapes, variations in more than one of these properties create interpretational ambiguities and challenges in relating  $EC_a$  to a specific soil property. Because of equivalence, a functional analysis of each soil-landscape or management units is required to decipher the exact site-specific causes of EMI variability (Sommer et al., 2003).

Electromagnetic induction has significant advantages over conventional soil survey techniques because of its speed and ease of use. Maps of  $EC_a$  can provide higher levels of resolution than soil maps prepared with conventional methods (Jaynes, 1995). Electromagnetic induction provides a larger number of observations and more comprehensive coverage of sites than traditional soil survey methods. Maps of  $EC_a$  appear to be reasonable facsimiles of soil maps. In many areas, spatial  $EC_a$  patterns corresponded well with the soil patterns shown on soil survey maps (Jaynes, 1995).

Electromagnetic induction has been used to assess depths to claypans (Sudduth et al., 1995; Doolittle et al., 1994; Stroh et al., 1993; Sudduth and Kitchen, 1993), soil drainage classes (Kravchenko et al., 2002), and soil salinity (Rhoades and Corwin, 1981); and to measure soil water content (Sheets and Hendrickx, 1995; Kachanoski et al., 1988), clay content (Sommer et al., 2003; William and Hoey, 1987); cation exchange capacity and exchangeable Ca and Mg (McBride et al., 1990), soil organic carbon (Jaynes, 1996), field-scale leaching rates of solutes (Slavich and Yang, 1990), and herbicide partition coefficients (Jaynes et al., 1994). Electromagnetic induction has also been used as a soil-mapping tool to assist precision agriculture (Jaynes, 1995; Jaynes et al., 1995; Sudduth et al., 1995) and to evaluate soil properties that affect yields (Johnson et al., 2001). In these studies,  $EC_a$  was either directly related to the parameter under investigation or the parameter (such as soil organic carbon) was associated with changes in a property (soluble salt, moisture and clay contents) that EMI measures.

Since the late 1970s, GPR has been used in the United States to assess properties of soils which affect their use, management, and classification. In 1979, the use of GPR for soil surveys was successfully demonstrated in a study conducted in Florida (Benson and Glaccum, 1979; Johnson et al., 1979). Because of the prevalence of sandy soils with favorable characteristics and contrasting subsoil, GPR has been used extensively in Florida to update soil surveys (Schellentrager et al., 1988). In other areas, the principal uses of GPR have been to evaluate soil properties and to estimate the variability and taxonomic composition of soil map units.

In upland areas such as found in Berks County, Pennsylvania, GPR is ideally suited to provide information concerning the depth and structure of the underlying parent rock. Ground penetrating radar has been used extensively to chart bedrock depths (Collins et al., 1989; Davis and Annan, 1989), changes in rock type (Davis and Annan, 1989), characterize fractures and joint patterns (Porsani et al., 2005; Nascimento da Silva et al., 2004; Lane et al., 2000; Pipan et al., 2000), cavities, sinkholes, and fractures in limestone (Al-fares et al., 2002; Pipan et al., 2000) and faults (Demagnet et al., 2001; Meschede et al., 1997). In mining and quarry operations, GPR has been used to detect geologic hazards and to optimize extraction costs (Singh and Chauhan, 2002; Grodner, 2001; and Molinda et al., 1996). Ground-penetrating radar has been used in hydrogeologic investigations to study the structure (fractures, unloading or exfoliation joints, bedding and stress planes, cavities, etc.) of the underlying bedrock (Porsani et al., 2005; Al-fares et al., 2002; Singh and Chauhan, 2002). Ground-penetrating radar has revealed structural features (e.g., bedding and fracture planes, karstified zones, compacted and massive limestone, and conduits) in limestone, which influenced the infiltration of water (Al-fares et al., 2002).

### **Equipment:**

A Dualem-2 meter (Dualem Inc., Milton, Ontario) was used in this survey<sup>1</sup>. The operation of the Dualem-2 meter is described by Taylor (2000). The Dualem-2 meter consists of one transmitter and two receiver coils. One receiver and the transmitter provide a perpendicular (PRP) geometry. The other receiver provides a horizontal co-planar (HCP) geometry

<sup>1</sup> Manufacturer's names are provided for specific information; use does not constitute endorsement.

with the transmitter. The dual-geometry array of the Dualem-2 meter allows two depths to be measured simultaneously without rotating the coils. The meter is keypad operated and has about 1 megabyte of memory. The depth of penetration is “geometry limited” and dependent on the instrument’s intercoil spacing, coil or receiver geometries, and frequency. The Dualem-2 has a 2-m intercoil spacing between the transmitter and the two receivers. Lateral resolution is approximately equal to the intercoil spacing. The Dualem-2 meter operates at a fixed frequency (9,000 Hz). It has theoretical penetration depths of 1.3 and 3.0 m in the PRP and HCP geometries, respectively.



*Figure 1. A mobile EMI survey system with a Dualem-2 meter mounted in a cart traverses an area of Berks-Weikert complex, 15 to 25 % slopes in Leesport.*

The DAS70 Data Acquisition System (Geonics Limited, Mississauga, Ontario) was used with the EMI meters to record and store both  $EC_a$  and GPS data.<sup>2</sup> The acquisition system consists of an EMI meter, an Allegro field computer (Juniper Systems, North Logan, UT), and a Trimble AG114 GPS receiver (Trimble Navigation, Ltd., Sunnyvale, CA).<sup>2</sup> With the acquisition system, the EMI meter is keypad operated and measurements are automatically triggered.

To help summarize the results of this study, the SURFER for Windows (version 8.0) software (Golden Software, Inc., Golden, CO) was used to construct two-dimensional simulations.<sup>2</sup> Grids were created using kriging methods with an octant search.

The radar unit is the TerraSIRch Subsurface Interface Radar (SIR) System-3000 (Geophysical Survey Systems, Inc., North Salem, New Hampshire).<sup>2</sup> The use and operation of GPR is described by Daniels (2004). The SIR System-3000 consists of a digital control unit (DC-3000) with keypad, SVGA video screen, and connector panel. The SIR System-3000 weighs about 4.1 kg (9 lbs) and is backpack portable. With an antenna, this system requires two people to operate. A 200 MHz antenna was used in this study. All radar records were processed with the RADAN for Windows (version 5.0) software program (Geophysical Survey Systems, Inc., North Salem, New Hampshire).<sup>2</sup> Processing included setting the initial pulse to time zero, color transformation, distance and surface normalization, signal stacking, background removal, migration, and range gain adjustments.

<sup>2</sup> Manufacturer's names are provided for specific information; use does not constitute endorsement.

### Study Sites:

The two study sites are located in northwestern Berks County and in Major Land Resource Area 147 – *Northern Appalachian Ridge and Valley*. Sites are located at the Berks County Fairgrounds in Leesport, and in North Heidelberg Township near Mt Pleasant. These sites will be referred to as the *Fairgrounds* and *Blue Marsh* Sites, respectively.

At each sites, soil patterns are intricate. The soil map units recognized within these sites are listed in Table 1. The taxonomic classifications of these soils are listed in Table 2. All soils are well drained. The moderately deep Berks and shallow Weikert soils form in residuum weathered from shale and siltstone. The very deep Duffield and moderately deep Ryder soils form in residuum weathered from limestone and calcareous siltstone. In general, Duffield and Ryder soils have a slightly higher clay content and cation exchange capacity than Berks and Weikert soils.

**Table 1.**  
**Map Unit Legend for the Fairground and Blue Marsh Sites, Berks County, Pennsylvania.**

<b>Symbol</b>	<b>Map Unit Name</b>
BkB	Berks-Weikert, 3 to 8 % slopes
BkC	Berks-Weikert complex, 8 to 15 % slopes
BkD	Berks-Weikert complex, 15 to 25 % slopes
BkF	Berks-Weikert complex, 25 to 60 % slopes
DbB	Duffield silt loam, 3 to 8 % slopes
DfC	Duffield-Ryder silt loams, 8 to 15 % slopes
DfD	Duffield-Ryder silt loams, 15 to 25 % slopes
WeD	Weikert-Berks complex, 15 to 25 % slopes

**Table 2**  
**Taxonomic classifications of soils surveyed with EMI in Berks County, Pennsylvania.**

<b>Series</b>	<b>Taxonomic classification</b>
Berks	Loamy-skeletal, mixed, mesic Typic Dystrochrepts
Duffield	Fine-loamy, mixed, mesic Ultic Hapludalfs
Ryder	Fine-loamy, mixed, mesic Ultic Hapludalfs
Weikert	Loamy-skeletal, mixed, mesic Lithic Dystrochrepts

The Fairground Site is located on the north-facing slopes of a narrow ridgeline. The survey area was irregularly shaped and did not conform to field boundaries. The general location of the survey area is in the southwestern portion of the large cultivated fields shown in Figure 2. The underlying parent rock is the Lower Ordovician Epler formation (interbedded limestone and dolomite) and Hamburg sequence (limestone and shale). Soils on ridgeline formed in residuum weathered from shale, while soils on foot slopes formed in residuum weathered from limestone. Lower-lying foot slope areas are mapped as Duffield silt loam, 3 to 8 % slopes (DbB). Higher-lying back slope and summit areas include polygons of Berks-Weikert complex, 8 to 15 % slopes (BkC), and Berks-Weikert complex, 15 to 25 % slopes (BkD) (see Figure 1). A polygon of Weikert-Berks complex, 15 to 25 % slopes (WeD) extends into the survey area. However, most areas of this polygon were not surveyed with the mobile EMI surveying system because of steep slopes and trees (see Figure 2).

The Blue Marsh Site is located on a broad upland area of a ridge spur that slopes mostly to the north and south. The survey area was irregularly shaped and its boundaries conformed to field boundaries (see Figure 3). The underlying parent rock is the Lower Ordovician Hamburg sequence (limestone and shale). Soils formed in residuum weathered principally from limestone. Compared with the Fairground Site, slopes are gentler at the Blue Marsh Site. The site is dominated by several units of Duffield and Ryder soils. The less sloping summit area is dominated by Duffield silt loam, 3 to 8 % slopes (DbB). The more sloping back slope components of the spur are dominated by areas of Duffield-Ryder silt loams, 8 to 15 % slopes (DfC), and Duffield-Ryder silt loams, 15 to 25 % slopes (DfD).



Figure 2. Soil Map of the Fairground Site showing the approximate area surveyed with EMI (enclosed by green lines).

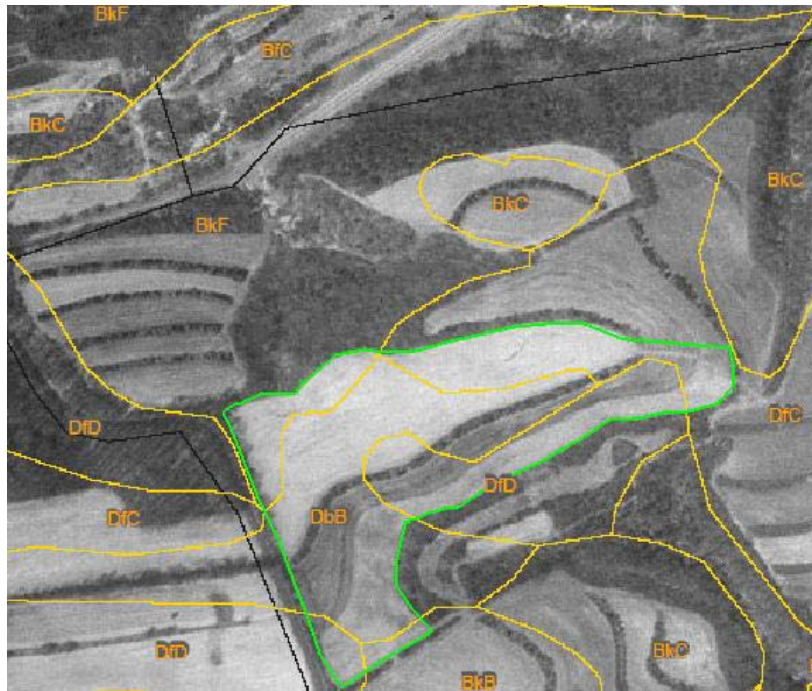


Figure 3. Soil Map of the Blue Marsh Site showing the fields surveyed with EMI (enclosed by green lines).

#### Field Methods:

A mobile EMI surveying system was used at each site. Compared with pedestrian surveys, larger data sets can be collected more quickly and effortlessly with mobile surveying systems equipped with global positioning systems (GPS) (Cannon et al. 1994; Freeland et al., 2002). In open fields that are greater than 1-ha, mobile surveying systems are more efficient and provide substantially greater data density than pedestrian surveys (Freeland et al., 2002). However, for smaller-sized fields

and in more inaccessible terrains, pedestrian surveying methods are more practical. The Dualem-2 meter was mounted on an EMI cart and towed behind a John Deere “Gator” 6x4 ATV (see Figure 1) <sup>1</sup>. To reduce the affects of ATV engine noise on EMI measurements, the Dualem-2 meter was separated from the ATV by fiberglass extension pole (see Figure 1). The Dualem-2 meter was positioned on the cart at a height of about 30-cm above the ground surface and operated in the continuous mode with geo-referenced  $EC_a$  measurements recorded at 1-sec intervals. As it is impractical to mount the GPS antenna above the EMI meter, slight positioning errors, or offsets, do exist in the data sets. Multiple traverses were completed with this system across each study site. Traverse lines were randomly spaced across each field. Measurements obtained in the field were not corrected to a reference temperature of 25° C.



*Figure 4. Survey flags marks the location of reference points along a GPR traverse line at the Fairground Site in Berks County, Pennsylvania.*

At each site, GPR traverse lines were laid out (see Figure 4). These lines were orientated perpendicular to slope contours and crossed different slope components. Traverse lines varied from 22- to 44-m in length. The origin (0-m distance mark) was located on the highest point on the lines. Along each line, survey flags were inserted in the ground at a 2-m interval and served as reference points. The elevation of each reference point was measured with a level and stadia rod. Elevations were not tied to a benchmark; the lowest reference point along a traverse line was chosen as the 0.0 m datum. Radar surveys were completed by pulling a 200 MHz antenna along each traverse line. As the antenna passed a flagged reference points, a vertical mark was impressed on the radar record.

## **Results:**

### **EMI -**

#### Fairground Site:

Table 3 lists the basic statistics for the EMI surveys. Each site was covered with a modest number of observations. In general,  $EC_a$  was low and relatively invariable across each site.

At the Fairground Site,  $EC_a$  averaged about 6.8 and 2.5 mS/m for measurements obtained in the deeper-sensing, HCP and the shallower-sensing, PRP geometries, respectively. In the horizontal coplanar geometry,  $EC_a$  ranged from 0.0 to 9.1 mS/m with a standard deviation of only about 1.0 mS/m. In the perpendicular geometry,  $EC_a$  ranged from 0.0 to 5.4 mS/m, with a standard deviation of only 0.8 mS/m. While soils and soil properties did vary across the Fairground Site, these differences did not significantly affect  $EC_a$ . The lack of noticeable changes in  $EC_a$  across this site attests to the similar

electromagnetic properties of the soils or equivalence. The low and essentially invariable  $EC_a$  at this site limits the effectiveness of EMI to delineate differences in soils and soil properties.

**Table 3**

	<b>Basic EMI Statistics for EMI surveys.</b>			
	<b>(Other than the number of observations, all values are in mS/m)</b>			
	<b>Fairground Site</b>		<b>Blue Marsh Site</b>	
	<b>HCP</b>	<b>PRP</b>	<b>HCP</b>	<b>PRP</b>
<b>Number</b>	1166	1166	2001	2001
<b>Mean</b>	6.76	2.51	7.61	4.32
<b>Standard Deviation</b>	1.05	0.85	1.25	1.16
<b>Minimum</b>	0.00	-0.01	0.00	0.00
<b>Maximum</b>	9.10	5.40	12.30	8.80
<b>25%-tile</b>	6.20	2.00	6.80	3.60
<b>75%-tile</b>	7.40	3.10	8.30	5.00

The mobile surveying system required the Dualem-2 meter be suspended at a height of about 30 cm above the ground surface. This resulted in a reduction in  $EC_a$  in both geometries because air occupies a portion of the volume that is sensed with the instrument. The instrument's response varies as a nonlinear function of depth (Sudduth et al., 2001). In the PRP geometry, the meter is most sensitive to the medium immediately beneath the coils (the air column between the meter and the ground). In the HCP geometry, the meter is most sensitive to the materials at a depth of about 80 cm (or 50 cm when the instrument is suspended at a height of 30 cm). Operating at low-induction numbers, when held at a height of 30 cm above the ground surface, the meter should theoretically experience a 15 % and 45% reduction in responses measured in the HCP and PRP geometries, respectively (McNeill, 1980). Because of the electrically resistive nature of these soils, any reduction in  $EC_a$  measured in PRP geometry is considered significant. Survey conducted in the PRP would provide more meaningful measurements if the meter were placed on or nearer the ground surface.

Figure 5 contains two-dimensional plots of  $EC_a$  measured with the Dualem-2 meter in the PRP (upper plot) and HCP (lower plot) geometries. In both plots, the isoline interval is 1 mS/m and the same color scale is used. It is generally not recommended to use isoline intervals less than 2-mS/m because of inference caused by system and background noise. Drift and background noise can produce slight errors in measurement (about 2 mS/m), which are often more noticeable in data set collected in areas of low  $EC_a$ . However, because of the lack of variability in  $EC_a$  across this site, an interval of 1 mS/m was used.

The spatial  $EC_a$  patterns shown on these plots are unremarkable. Data collected in the PRP geometry generally lacks well defined patterns that can be associated with systematic changes in soil and/or landscape components. In the deeper-sensing, HCP,  $EC_a$  patterns appear to conform to soil and landform components. Based on tacit knowledge of the site, spatial  $EC_a$  patterns, shown in the plot of HCP data, are associated with differences in soil depth, texture, and moisture contents. In Figure 5, an area of higher  $EC_a$  forms a broad pattern that trends in a northwesterly direction from the southeast to northwest corners of the site. This area conforms to a noticeable slope break and seepage area that forms a boundary between units of Weikert-Berks complex, 15 to 25 % slopes (WeD), and Berks-Weikert complex, 8 to 15 % slopes (BkC). This swale contains deeper and presumably moister soils. Indistinct, east-to-west trending, linear patterns in the northern portion of the site appear to follow the strike of the underlying bedrock. Differences in this portion of the site are attributed principally to differences in lithology and soil depth.

The low and invariable  $EC_a$  at the Fairground Site makes spatial patterns indistinct and interpretations ambiguous. This site is considered poorly suited to EMI.

#### Blue Marsh Site:

At the Blue Marsh Site,  $EC_a$  averaged about 7.6 and 4.3 mS/m for measurements obtained in the deeper-sensing, HCP and the shallower-sensing, PRP geometries, respectively. Apparent conductivity was higher and slightly more variable at the Blue Marsh Site than at the Fairgrounds Site. These differences are attributed to the dominance of limestone rather than shale at this site, and the greater averaged clay content and higher cation-exchange capacity of Duffield and Ryder soils at the Blue Marsh Site than the Berks and Weikert soils at the Fairground Site. At the Blue Marsh Site, in the HCP geometry,

$EC_a$  ranged from 0.0 to 12.3 mS/m, with a standard deviation of about 1.2 mS/m. In the PRP geometry,  $EC_a$  ranged of 0.0 to 8.8 mS/m, with a standard deviation of 1.2 mS/m.

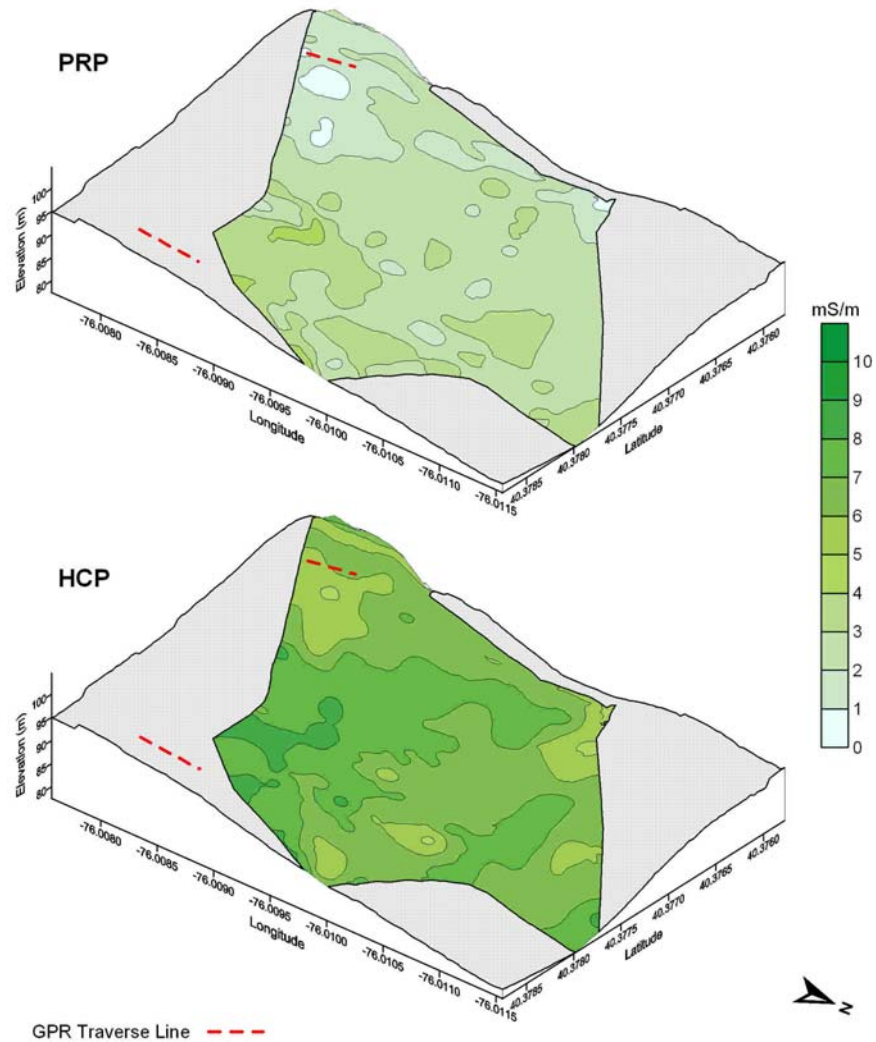


Figure 5. Plots of  $EC_a$  measured with the Dualem-2 meter in the perpendicular (upper plot) and the horizontal coplanar (lower plot) geometries at the Fairground Site.

Figure 6 contain two-dimensional plots of  $EC_a$  measured with the Dualem-2 meter in the PRP (upper plot) and HCP (lower plot) at the Blue Marsh Site. In each plot, the isoline interval is 2 mS/m and the same color scale is used. Apparent conductivity increased with increasing depth of observation ( $EC_a$  measured in the deeper sensing HCP was typically higher than the  $EC_a$  measured in the shallower sensing PRP). As the water table was below the depth of observation, this vertical trend is assumed to reflect the more conductive nature of the underlying limestone bedrock than the overlying soil. Within this site,  $EC_a$  was higher on lower-lying concave back slope surfaces than on higher-lying, convex shoulder and summit areas. This relationship is known as the *terrain effect* and is evident with EMI at most sites. In the eastern United States, differences in  $EC_a$  associated with landscape components principally reflect differences in soil depth, clay and moisture contents. In both geometries, the highest  $EC_a$  was measured in a swale, which is located in the southwestern portion of site. This swale receives seepage and runoff from adjoining slopes.

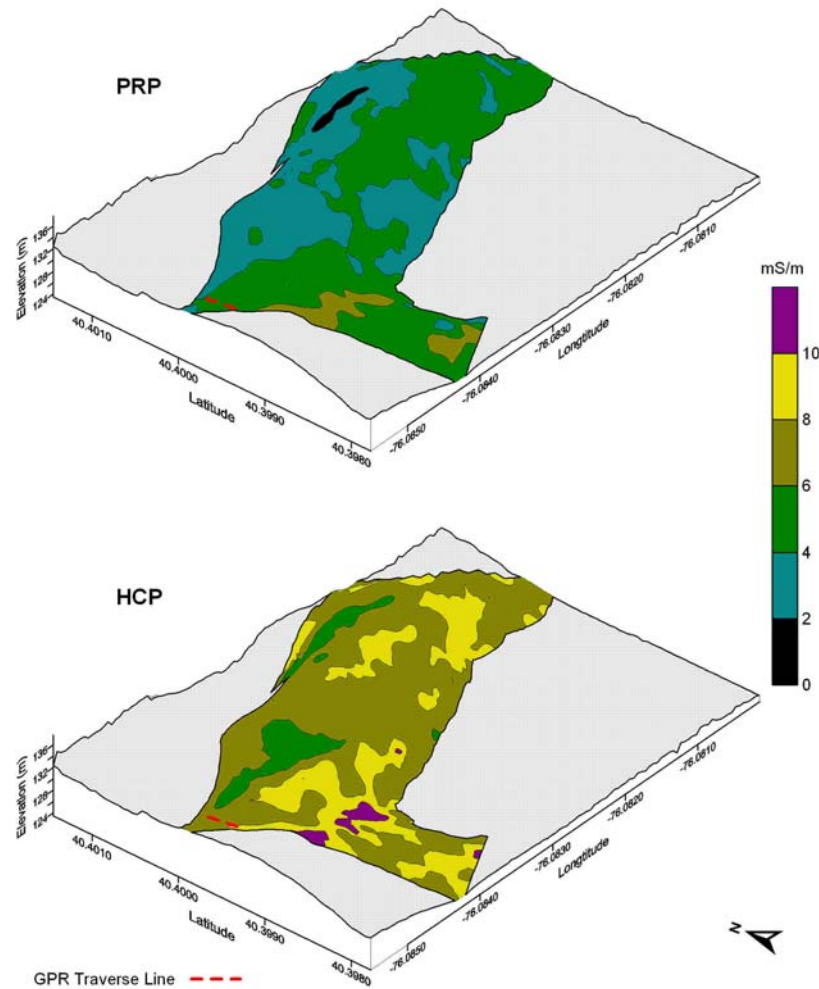


Figure 6. Plots of  $EC_a$  measured with the Dualem-2 meter in the perpendicular (upper plot) and the horizontal coplanar (lower plot) geometries at the Blue Marsh Site.

### GPR Surveys-

The approximate locations of GPR traverse lines discussed in this report are identified by segmented red lines in Figures 5 and 6.

#### Calibration:

Ground-penetrating radar is a time scaled system. This system measures the time taken by electromagnetic energy to travel from an antenna to an interface (e.g., soil horizon, stratigraphic layer, parent rock) and back. To convert the travel time into a depth scale, either the velocity of pulse propagation or the depth to a reflector must be known. The relationships among depth (D), two-way pulse travel time (T), and velocity of propagation (V) are described in the following equation (Daniels, 2004):

$$V = 2D/T \quad [1]$$

The velocity of propagation is principally affected by the relative dielectric permittivity ( $E_r$ ) of the profiled material(s) according to the equation (Daniels, 2004):

$$E_r = (C/V)^2 \quad [2]$$

In equation [2],  $C$  represents the velocity of propagation in a vacuum (0.298 m/ns). Velocity is expressed in meters per nanosecond (ns). The amount and physical state (temperature dependent) of water have the greatest effect on the  $E_r$  of earthen materials. Based on the depth to a known reflector, the  $E_r$  was estimated to be 8.2 in the upper part of the soil profile. This resulted in a propagation velocity of 0.104 m/ns. Substituting into Equation [1] a scanning-time of 65 ns and a propagation velocity of 0.10 m/ns, the maximum penetration depth was (assuming a constant velocity) about 3.4 m.

#### Interpretation:

Figure 7 contains a 28-m portion of a radar record which was collected in area of Weikert-Berks complex, 15 to 25 % slopes (WeD) at the Fairgrounds Site. A picture of this traverse line is shown in Figure 4. This line was 44-m long. The line is orientated perpendicular to the slope contours and passed between the areas of rock outcrops shown in Figure 4. In Figure 5, this GPR traverse line is the eastern-most line and is located outside the EMI survey area.

On the radar record shown in Figure 7, the vertical or depth scale is expressed in meters. The radar record has been *surface normalization*, a post-processing procedure that assigns elevations to each reference point so that the radar records can be corrected for changes in surface topography. Surface normalized presentations aid soil/landscape correlations and improves interpretations. In addition, surface normalization contributes to the proper geometric reconstruction of the various structural elements (e.g., discontinuities, bedding and fracture planes) of the underlying bedrock.

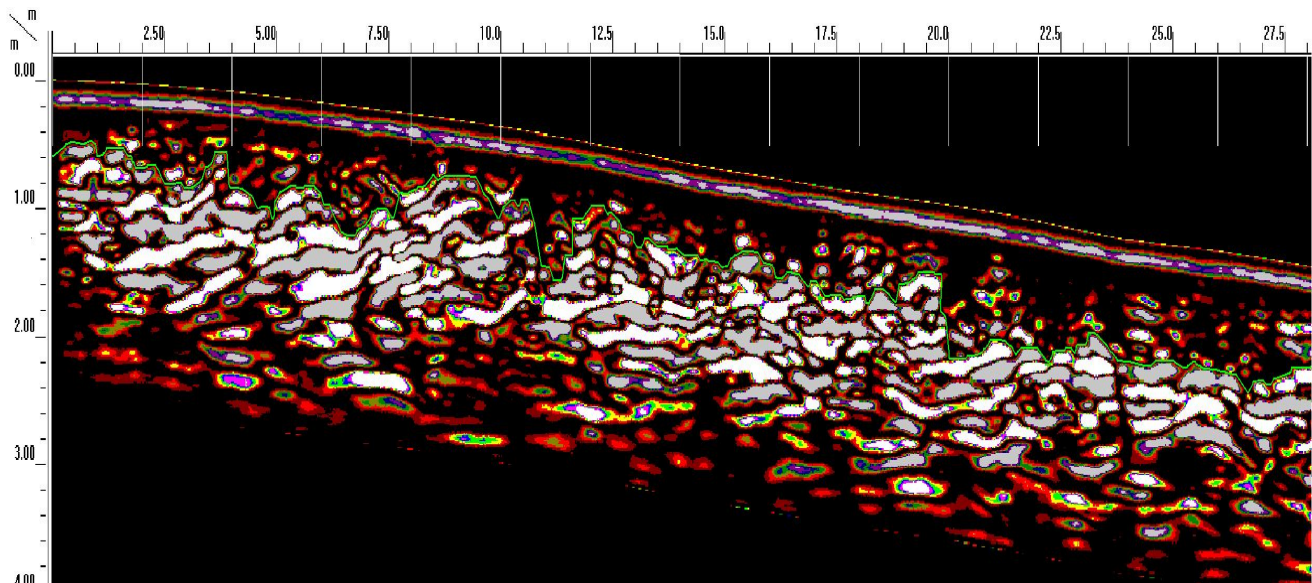


Figure 7. Representative radar record from an area of Weikert-Berks complex, 15 to 25 % slopes.

The bedrock surface affords an identifiable high amplitude radar reflection. A green line has been used in Figure 7 to identify the interpreted bedrock surface. This surface appears highly irregular and segmented. Above the bedrock surface are point reflectors from larger rock fragments in the Berks and Weikert soils. In rocks, high amplitude radar reflections are associated with water filled joints, fractures, and structural planes (Lane et al., 2000; Buursink and Lane, 1999; Olhoeft, 1998; Grasmueck, 1994). In Figure 7, the slightly dipping sub-parallel reflectors evident below the bedrock surface represent bedding planes in the shale. These reflectors vary spatially in form and signal amplitude. Variations in signal amplitudes are attributed principally to differences in moisture contents along bedding planes. In Figure 7, if moisture flows along these surfaces, the flow is to the left (south) and into the landform. The segmented and disjointed appearance of bedrock reflectors suggests that the underlying shale is highly fractured. High scattering losses occur in highly fractured rocks and limit the penetration depth and effectiveness of higher frequency antennas.

Figure 8 contains an 18-m portion of a radar record which was collected in area of Berks- Weikert complex, 25 to 60 % slopes (BkF) at the Blue Marsh Site. The line is orientated perpendicular to the slope contours. The approximate location of this traverse line is shown in Figure 6.

Once again, the bedrock surface affords an identifiable, high amplitude radar reflection. A green line has been used in Figure 8 to identify the interpreted bedrock surface. In most portions of this radar record, the soil/bedrock interface

produces a high amplitude reflection, which is readily discernible (in Figure 8, between 20 and 28-m marks). In some portions of this radar record, reflections from the bedrock surface are lower in amplitude and highly segmented and irregular (in Figure 8, between 14 and 17-m marks). In these portions of radar records, the soil/bedrock interface is more difficult to follow and interpretations are more ambiguous.

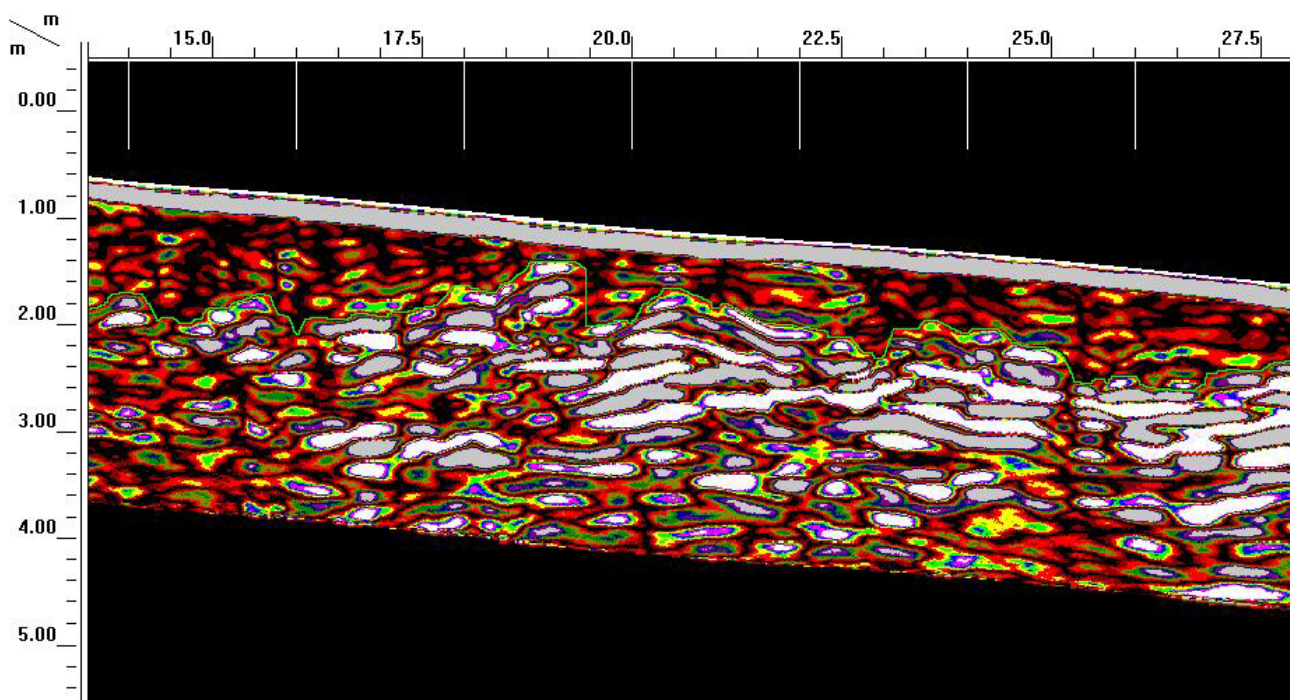


Figure 8. Radar record from an area of Berks-Weikert complex, 25 to 60 % slopes at the Blue Marsh Site.

Table 3 summarizes the frequency distribution of soils by soil depth classes along the traverse lines completed at the Fairgrounds and Blue Marsh Sites. Each traverse line is identifying by a map unit symbol. At the Fairground Site, radar traverses were completed in areas of Berks-Weikert complex, 8 to 15 % slopes (BkC) and Weikert-Berks complex, 15 to 25 % slopes (WeD). Two traverses were completed in an area of BkC. These traverse lines were 44 and 22 m long and contained 23 and 12 observations, respectively. Soils along these lines are dominantly moderately deep and shallow to bedrock. Depths to bedrock ranged from 38 to 110 cm along these lines. The traverse completed in an area of WeD was 44 m long and contained 23 observations. Soils along this line are dominantly moderately deep and deep to bedrock. The averaged depth to bedrock along this line was 90 cm with a range of 45 to 125 cm. At the Blue Marsh Site, a radar traverse was completed in an area of Berks-Weikert complex, 25 to 60 % slopes (BkF). This traverse was 40-m long and contained 21 observations. Soils along this line are dominantly moderately deep and deep to bedrock. The averaged depth to bedrock along this line was 92 cm with a range of 60 to 123 cm.

**Table 3.**  
**Frequency Distribution of Bedrock Depths along GPR Traverse Lines.**

Depth Class-----	Map Units			
	BkC	BkC	WeD	BkF
Shallow -----	0.17	0.08	0.09	0.00
Moderately Deep -----	0.78	0.67	0.57	0.67
Deep-----	0.04	0.25	0.35	0.33
Very Deep-----	0.00	0.00	0.00	0.00

**References:**

- Al-fares, W., M. Bakalowicz, R. Guerin, and M. Dukhan. 2002. Analysis of the karst aquifer structure of the Lamalou area (Herault, France) with ground penetrating radar. *Journal of Applied Geophysics* 51: 97-106.
- Benson, R. and R. Glaccum. 1979. Test Report; The application of ground-penetrating radar to soil surveying for National Aeronautical and Space Administration (NASA). Technos Inc. Miami, Florida.
- Buursink, M.L., and J. W. Lane. 1999. Characterizing fractures in a bedrock outcrop using ground-penetrating radar at Mirror Lake, Grafton County, New Hampshire. 769-776 pp. IN: Morganwalp, D.W., and Buxton, H.T. (editors), U.S. Geological Survey Toxic Substances Hydrology Program--Proceedings of the Technical Meeting, Charleston, South Carolina, March 8-12, 1999--Volume 3 of 3--Subsurface Contamination from Point Sources: U.S. Geological Survey Water-Resources Investigations Report 99-4018C.
- Cannon, M. E., R. C. McKenzie, and G. Lachapelle. 1994. Soil salinity mapping with electromagnetic induction and satellite-based navigation methods. *Canadian Journal of Soil Science*: 335-343.
- Collins, M. E., J. A. Doolittle, and R. V. Rourke. 1989. Mapping depth to bedrock on a glaciated landscape with ground-penetrating radar. *Soil Sci. Soc. Am. J.*, 53(3): 1806-1812.
- Daniels, D. J. 2004. *Ground Penetrating Radar*; 2<sup>nd</sup> Edition. The Institute of Electrical Engineers, London, United Kingdom.
- Davis, J. L., and A. P. Annan. 1989. Ground-penetrating radar for high-resolution mapping of soil and rock stratigraphy. *Geophysical Prospecting*, 37: 531-551.
- Demant, D., L. G. Evers, H. Teerlynck, B. Dost, and D. Jongmans. 2001. Geophysical investigations across the Peel boundary fault (The Netherlands) for a paleoseismological study. *Netherlands Journal of Geosciences* 80 (3-4): 119-127.
- Doolittle, J. A., K. A. Sudduth, N. R. Kitchen, and S. J. Indorante. 1994. Estimating depth to claypans using electromagnetic inductive methods. *J. Soil and Water Conservation* 49(6): 552-555.
- Freeland, R. S., R. E. Yoder, J. T. Ammons, and L. L. Leonard. 2002. Mobilized surveying of soil conductivity using electromagnetic induction. *American Society of Agricultural Engineers. Applied Engineering in Agriculture* 18(1): 121-126.
- Grodner, M. 2001. Using ground penetrating radar to quantify changes in fracture pattern associated with a simulated rockburst experiment. *Journal of the South African Institute of Mining and Metallurgy*. 101(5): 261-266.
- Grasmueck, M. 1994. Application of seismic processing techniques to discontinuity mapping with ground-penetrating radar in crystalline rock of the Gotthard Massif, Switzerland. 1135-1149 pp. IN: *Proceeding of the Fifth International Conference on Ground Penetrating Radar*. Waterloo Centre for Groundwater Research and Canadian Geotechnical Society. June 12-16 1994, Kitchner, Ontario, Canada.
- Jaynes, D. B. 1995. Electromagnetic induction as a mapping aid for precision farming. 153-156 pp. IN: *Clean Water, Clean Environment, 21st Century: Team Agriculture. Working to Protect Water Resources*. Kansas City, MO. 5 to 8 March 1995.
- Jaynes, D.B. 1996. Improved Soil Mapping using Electromagnetic Induction Surveys. 169-179 pp. *Proc. 3rd Int. Conf. on Precision Agriculture*, Minneapolis, June 23-26, 1996. ASA-CSSA-SSSA. Madison, WI.
- Jaynes, D. B., and T. S. Colvin. 1997. Spatiotemporal variability of corn and soybean yields. *Agronomy J.* 89(1): 30-37.
- Jaynes, D. B., J. M. Novak, T. B. Moorman, and C. A. Cambardella. 1994. Estimating herbicide partition coefficients from electromagnetic induction measurements. *J. Environmental Quality*. 24:36-41.

- Jaynes, D. B., T. S. Colvin, and J. Ambuel. 1995. Yield mapping by electromagnetic induction. 383-394 pp. IN: Robert, P. C., R. H. Rust, and W. E. Larson (editors). Proceedings of Second International Conference on Precision Management for Agricultural Systems. Minneapolis, MN. March 27-30, 1994. American Society of Agronomy, Madison, WI.
- Johnson, C. K., J. W. Doran, H. R. Duke, B. J. Wienhold, K. M. Eskridge, and J. F. Shanaha. 2001. Field-scale conductivity mapping for delineating soil condition. *Soil Sci. Soc. Am. J.* 65:1829-1837.
- Johnson, R. W., R. Glaccum, and R. Wojtasinski. 1979. Application of ground penetrating radar to soil survey. *Soil and Crop Science Society of Florida Proceedings* 39: 68-72.
- Kachanoski, R. G., E. G. Gregorich, and I. J. van Wesenbeeck. 1988. Estimating spatial variations of soil water content using noncontacting electromagnetic inductive methods. *Can. J. Soil Sci.* 68:715-722.
- Kravchenko, A. N., G. A. Bollero, R. A. Omonode, and D. G. Bullock. 2002. Quantitative mapping of soil drainage classes using topographical data and soil electrical conductivity. *Soil Sci. Soc. Am. J.* 66:235-243.
- Lane Jr., J. W., M. L. Buursink, F. P. Haeni, and R. J. Versteeg. 2000. Evaluation of ground-penetrating radar to detect free-phase hydrocarbons in fractured rocks – results of numerical modeling and physical experiments. *Ground Water*, 38(6): 929-938.
- McBride, R. A., A. M. Gordon, and S. C. Shrive. 1990. Estimating forest soil quality from terrain measurements of apparent electrical conductivity. *Soil Sci. Soc. Am. J.*, 54:290-293.
- McNeill, J. D. 1980. Electromagnetic terrain conductivity measurement at low induction numbers. Technical Note TN-6. Geonics Limited, Mississauga, Ontario.
- Meschede, M., U. Asprion, and K. Reicherter. 1997. Visualization of tectonic structures in shallow-depth high-intensity ground penetrating radar (GPR) profiles. *Terra Nova* 9(4): 167-170.
- Molinda, G. M., W. D. Monaghan, G. L. Mowrey, and G. F. Persetic. 1996. Using ground penetrating radar for roof hazard detection in underground mines. USDOE. Pittsburgh Research Center, RI 9625.
- Nascimento da Silva, C. C., W. E. de Medeiros, E. F. Jarmin de Sa, and P. X. Neto. 2004. Resistivity and ground-penetrating radar images of fractures in a crystalline aquifer: a case study in Caicara farm – NE Brazil. *Journal of Applied Geophysics* 56: 295-307.
- Olhoeft, G. 1998. Electrical, magnetic, and geometric properties that determine ground penetrating radar performance. 177-182 pp. IN: Plumb, R. G. (editor) Proceedings of the Seventh International Conference on Ground-Penetrating Radar. May 27 to 30, 1998, Lawrence, Kansas. Radar Systems and Remote Sensing Laboratory, University of Kansas.
- Pipan, M., L. Baradello, E. Forte, and A. Prizzon. 2000. GPR study of bedding planes, fractures and cavities in limestone. 682-687 pp. IN: Noon, D. (editor) Proceedings Eight International Conference on Ground-Penetrating Radar. May 23 to 26, 2000, Goldcoast, Queensland, Australia. The University of Queensland.
- Porsani, J. L., V. R. Elis, and F. Y. Hiodo. 2005. Geophysical investigations for the characterization of fractured rock aquifer in Itu, SE Brazil. *Journal of Applied Geophysics* 57: 119-128.
- Rhoades, J. D., and D. L. Corwin. 1981. Determining soil electrical conductivity-depth relations using an inductive electromagnetic soil conductivity meter. *Soil Sci. Soc. AM. J.* 45: 255-260.
- Schellentrager, G. W., J. A. Doolittle, T. E. Calhoun, and C. A. Wettstein. 1988. Using ground-penetrating radar to update soil survey information. *Soil Science Society of America J.* 52:746-752.
- Sheets, K. R., and J. M. H. Hendrickx. 1995. Noninvasive soil water content measurements using electromagnetic induction. *Water Resources Research* 31: 2401-2409.

- Singh, K. K. K., and R. K. S. Chauhan. 2002. Exploration of subsurface strata conditions for a limestone mining area in India with ground-penetrating radar. *Environmental Geology* 41: 966-971.
- Slavich, P.G., and J. Yang. 1990. Estimation of field scale leaching rates from chloride mass balance and electromagnetic induction measurements. *Irrig. Sci.* 11:7-14.
- Sommer, M., M. Wehrhan, M. Zipprich, U. Weller, W. zu Castell, S. Ehrich, B. Tandler, and T. Selige. 2003. Hierarchical data fusion for mapping soil units at field scale. *Geoderma* 112: 179-196.
- Stroh, J., S. R. Archer, L. P. Wilding, and J. Doolittle. 1993. Assessing the influence of subsoil heterogeneity on vegetation patterns in the Rio Grande Plains of south Texas using electromagnetic induction and geographical information system. College Station, TX. *The Station* (Mar 93): 39-42.
- Stafford, J. V. 2000. Implementing precision agriculture in the 21<sup>st</sup> Century. *J. Agric. Engineering Research* 76: 267-275.
- Sudduth, K. A., and N. R. Kitchen, 1993. Electromagnetic induction sensing of claypan depth. Paper No. 93-1550. Presented at the December 1993, Winter Meetings of the American Society of Agricultural Engineers. St. Joseph, MI.
- Sudduth, K. A., S. T. Drummond, and N. R. Kitchen. 2001. Accuracy issues in electromagnetic induction sensing of soil electrical conductivity for precision agriculture. *Computers and Electronics in Agriculture* 31: 239-264.
- Sudduth, K. A., N. R. Kitchen, D. H. Hughes, and S. T. Drummond. 1995. Electromagnetic induction sensing as an indicator of productivity on claypan soils. pp. 671-681. IN: Robert, P. C., R. H. Rust, and W. E. Larson (editors). *Proceedings of Second International Conference on Precision Management for Agricultural Systems*. Minneapolis, Minnesota. March 27-30, 1994. American Society of Agronomy, Madison, WI.
- Taylor, R. S. 2000. Development and applications of geometric-sounding electromagnetic systems. Dualem Inc., Milton Ontario.
- William, B. G., and D. Hoey. 1987. The use of electromagnetic induction to detect the spatial variability of the salt and clay contents of soils. *Australian J. Soil Research* 25: 21-27.